Extended Abstracts of the 1991 International Conference on Solid State Devices and Materials, Yokohama, 1991, pp. 329-331 **PC3-5**

MBE Growth of AlGaAs/GaAs Vertical Cavity Surface Emitting Lasers and the Performance of PIN/VCSEL Integrated Structures

Y.H. Wang, G. Hasnain+, K. Tai+, J.D. Wynn+, B.E. Weir+, K.D. Choquette+, and A.Y. Cho+

Department of Electrical Engineering,
National Cheng-Kung University, Tainan, Taiwan, ROC
+AT&T Bell Laboratories, Murray Hill, NJ 07974, USA

All molecular beam epitaxy grown planar top emitting AlGaAs/GaAs multi-quantum well lasers were fabricated and characterized. The vertical cavity surface emitting laser (VCSEL) consists of GaAs/$Al_{0.2}Ga_{0.8}As$ (100/80 Å) quantum wells sandwiched between two two-step doped distributed Bragg reflector. Gain-guided VCSELs operate continuous wave up to 90 ^{o}C with a characteristics temperature of 210 ^{o}K and can be modulated at frequency above 5 GHz. Thresholds as low as 2 mA and CW powers more than 2 mW were obtained at room temperature.

Monolithic integration of a PIN photodetector on top of the VCSEL is also demonstrated and discussed. The integrated photodetector shows a linear response to the laser emission with an effective responsitivity of 0.25 A/W.

1. INTRODUCTION

Vertical cavity surface emitting lasers with unique features, such as low divergence output, inherently single longitudinal mode operation, high 2-dimensional packing density for arrays and wafer scale testing capability, are attractive for a wide variety of device applications[1-6]. All epitaxial semiconductor VCSELs for the ease of fabrication, good compatibility and ease of integration with other components have many advantages over those of ex-situ reflector deposition[1-3]. However, the drawback of the all epitaxial design is that the current flow must be through a p-doped distributed Bragg reflector (DBR). Due to the interfacial barriers in the valance band of such a structure, the induced resistance gives a sizeable heating effect. To reduce the resistance, the effects of the DBR structures were studied[7]. Low operating voltage is then achieved. The compatibility of all epitaxial VCSELs with the photodetector makes the "in-situ" monitor of laser output power possible. The purpose of this paper is to demonstrate the performance of VCSELs and the realization of PIN/VCSEL integrated structures.

2. EXPERIMENTAL

Two Ga and two Al cells in a Riber-2300 molecular beam epitaxy system were used to achieve the required two-step mirror profiles as shown in Fig. 1(a) for the reduction of heating effect induced by p-DBR. Each period of the DBR structure contains $Al_{0.14}Ga_{0.86}As$ (417 Å), $Al_{0.4}Ga_{0.6}As$ (100 Å), $Al_{0.7}Ga_{0.3}As$ (100 Å), AlAs (506 Å), $Al_{0.7}Ga_{0.3}As$ (100 Å) and $Al_{0.4}Ga_{0.6}As$ (100 Å). The inter-layers, $Al_{0.4}Ga_{0.6}As$ (100 Å) and $Al_{0.7}Ga_{0.3}As$, (100 Å), can effectively reduce the barrier to lower barrier height of the interface and reduce the series resistance[7]. The cladding layer of $Al_xGa_{1-x}As$ is about 2150 A with x graded from 0.6 to 0.3. One-third of the confinement layer near the active region is undoped, and the rest is doped to $1x10^{18}$ cm^{-3} to reduce the free carrier absorption. The active region contains 4 quantum wells of $Al_{0.2}Ga_{0.8}As$/GaAs (80/100 Å). Typically, the bottom n-type DBR consists of 29.5 periods with a doping concentration of $1x10^{18}$ cm^{-3}. Top p-type DBR is a 20-period with a doping concentration of $3x10^{-18}$ cm^{-3} in the first 5 periods, then increase to $5x10^{18}$ cm^{-3}. Finally, the concentration is increased to $5x10^{19}$ cm^{-3} near the surface layer of $Al_{0.14}Ga_{0.86}As$ to facilitate the ohmic contact[8,9]. Additional i-GaAs absorption layer (1/2λ thick) and n-AlGaAs (1λ thick) were grown on top of VCSEL as the PIN photodetector.

The laser structures were first examined with the refelectivity measurement using an Anritsu MS9001B optical spectrum analyzer. Fabry-Perot resonance shown as only a clear dip in the stop band on account of the extremely short optical cavity in good agreement with the calculation can be seen. Then, 300 KeV protons in a dose of $1x10^{15}$ cm^{-2} are implanted with the 10 um or 15 um-diameter windows protected by a thick photoresister to provide the later current confinement. Reactive ion etching was used to obtain the vertical walls at the annular contact with no under-cutting at metal edges of the PIN photodetector. The cross-sectional view of the integrated structure is shown in Fig.1(b).

3. RESULTS AND DISCUSSIONS

Figure 2 shows the output power-current characteristics of typical such gain-guided VCSELs operated at various temperatures. More than 2 mW of coherent power is emitted by these VCSELs at room temperature in a single longitudial mode near 860 nm. The line width is 0.2 Å limited by the system resolution. The side mode ratio is larger than 50dB [10]. The threshold current as low as 2.1 mA for these 15 um diameter VCSELs has been achieved. The emission up to 0.6 mW is truly a TEM_{00} mode giving a diffraction circular far-field pattern with a 7.8^{o} full width half maximum. The VCSELs continue to lase CW as the heat sink temperature is raised beyond 90 ^{o}C. This improvement results from the reduced heat effect by using the tailored doping profile. The characteristic temperature T_o of laser diodes is about 210 ^{o}K. T_o as high as 310 ^{o}K was also observed in a three quantum well lasers[11]. The uniformity of the threshold, shown in Fig.3, over 0.75 cm wide region with some variations is seen. The varition of the corresponding emitted wavelength is larger 200 A. This may limit the applications of the arrays.

The measured intrinsic frequency response of the VCSELs to small signal amplitude modulation for various optical power is shown in Fig.4. For a 0.5 mW output, a 3 dB bandwidth of 5.4 GHz is obtained. The frequency response as a function of output power could be related to as $f_r / \sqrt{P}$ =5.5 GHz $mW^{-0.5}$ which suggests that the gain saturation effects are negligible up to output power of 0.5 mW corresponding to an estimated internal power of ~ 50 mW[12].

High series resistance is still observed in the PIN/VCSEL structure due to the implanted DBR strutcure which current must funnel in from the 30 µm inner diameter p-contacts into the central 15 µm diameter un-implanted gain region. The VCSELs under forward bias lase CW at room temperature in a single longitudinal and transverse mode at 850 nm with a threshold of 3.2 mA. The typical L-I curve is shown in Fig.5. Due to the absorption of light in the i-GaAs layer of the PIN photodetector, the light output power is much less than those of discrete VCSELs. The roll-over in the L-I characteristics above 4.5 mA is due to excessive heating in the DBR structure. The corresponding photocurrent of the PIN detector is also shown in Fig.5. Clear onset photocurrent is observed when the injected current of VCSEL reaches 3.2 mA indicating the onset of lasing. The photodetector thus samples a portion of the laser output and is equivalent to replacing an external beam-splitter in front of the laser to monitor the power. The integrated photodetector shows a linear response to the laser emission with an effectivity responsity of 0.25 A/W. The structure could dynamically monitor the output power of the lasers. Detialed analysis and improvement of the PIN/VCSEL integrated structure will be discussed elsewhere[9].

4. CONCLUSION

In conclusion, we have fabricated the all molecular beam epiatxy grown AlGaAs/GaAs quantum-well vertical cavity top emitting lasers and the monolithically integrated PIN/VCSEL structure. High temperature CW operation up to 90 ^{o}C with a characteristic temperature of 210 ^{o}K is obtained. High frequency operation beyond 5 GHz is also possible. The threshold of 2mA with an output power larger than 2 mW has been achieved. The integrated PIN photodetector shows a linear response to the laser emission with an effective responsitivity of 0.25 W/A.

Acknowledgements: The work done at National Cheng-Kung University was partly supported by the National Science Council under Contracts No. NSC79-0417-E006-02 and NSC80-0404-E006-55. The author (Y.H.) would like to acknowledge the helpful discussion and assistance of Drs. N.K. Dutta, R.J. Fischer, L.W. Tu, S.N.G. Chu, Y.K. Chen, M. Hong, and J. Gamelin.

REFERENCES

1) K. Iga, F. Koyama, and S. Kinoshita, IEEE J. Quantum Electron, 24(1988) 1845.
2) F. Koyama, S. Kinoshita, and K. Iga, Appl. Phys. Lett., 55(1989) 221.
3) A. Ibaraki, K. Kawashima, K. Furusawa, T. Ishikawa, Y. Ymaguchi, and T. Niina, Jpn. J. Appl. Phys., 28(1989) L667.
4) J.L. Jewell, A. Scherer, S.L. McCall, Y.H. Lee, S.J. Walker, J.P. Harbison and L.T. Florez, Electron Lett., 25(1989) 1123.
5) K. Tai, R.J. Fischer, C.W. Seabury, N.A. Olsson, T-C.D. Huo, Y. Ota, and A.Y. Cho, Appl. Phys. Lett., 55(1989) 2473.
6) Y.H. Wang, K. Tai, J.D. Wynn, M. Hong, R.J. Fischer, J.P. Mannarerts, and A.Y. Cho, IEEE Photonics Tech. Lett., 2(1990) 456
7) K. Tai, L. Yang, Y.H. Wang, J.D. Wynn, and A.Y. Cho, Appl. Phys. Lett., 56(1990) 2496
8) Y.H. Wang, K. Tai, Y.F. Hsieh, S.N.G. Chu, J.D. Wynn, and A.Y. Cho, Appl. Phys. Lett., 57(1990) 1613.
9) G. Hasnain, K. Tai, Y.H. Wang, J.D. Wynn, K.D. Choquette, B.E. Weir, N.K. Dutta,and A.Y. Cho, to be published.

10)G.H. Hasnain, K. Tai, L. Yang, Y.H. Wang, R.J. Fischer, J.D. Wynn, B.E. Weir, N.K. Dutta, and A.Y. Cho, J. Quantum Electron. June, 1991.
11)L.W. Tu, Y.H. Wang, E.F. Schubert, B. Weir, G. Zydzik and A.Y. Cho, Electron. Lett., 27(1991) 457.
12)G. Hasnai, K. Tai, N.K. dutta, Y.H. Wang, J.D. Wynn, B.E. Weir, and A.Y. Cho, to be published. .

(a)

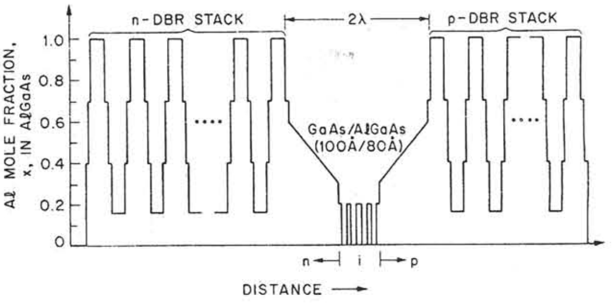

(b)

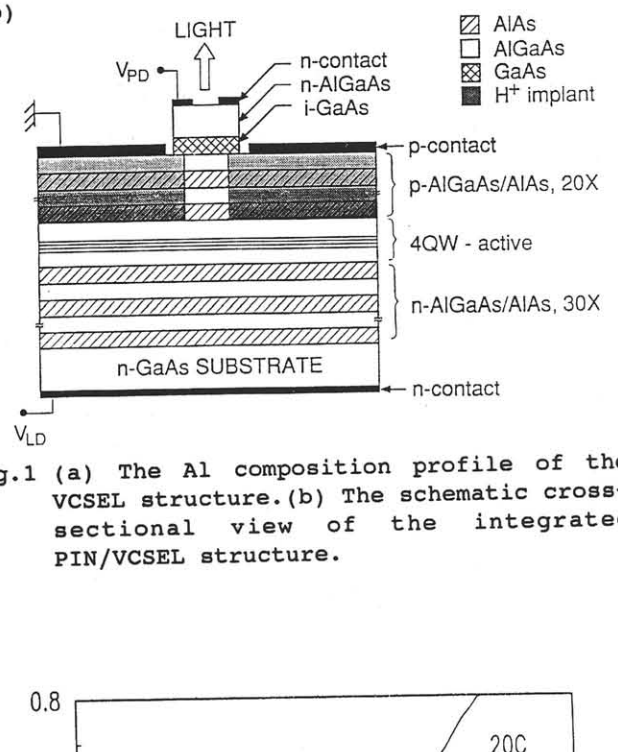

Fig.1 (a) The Al composition profile of the VCSEL structure.(b) The schematic cross-sectional view of the integrated PIN/VCSEL structure.

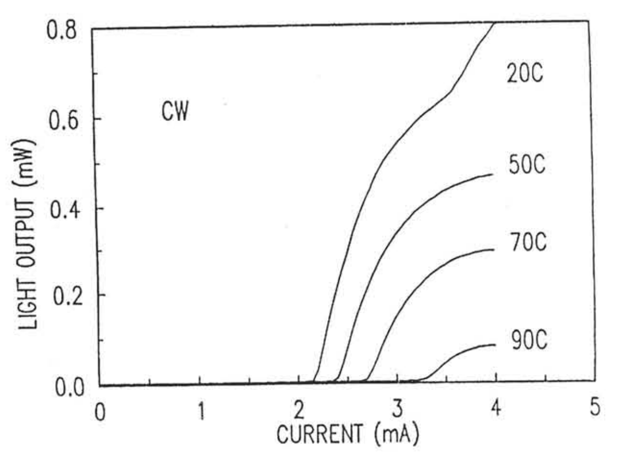

Fig.2 The typical L-I characteristics of the VCSELs. The corresponding characteristic temperature is 210 ^{o}K.

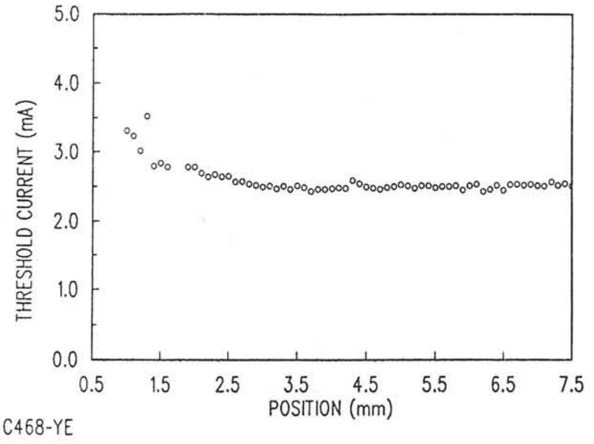

Fig.3 The uniformity of the threshold current over 0.75 cm wide region.

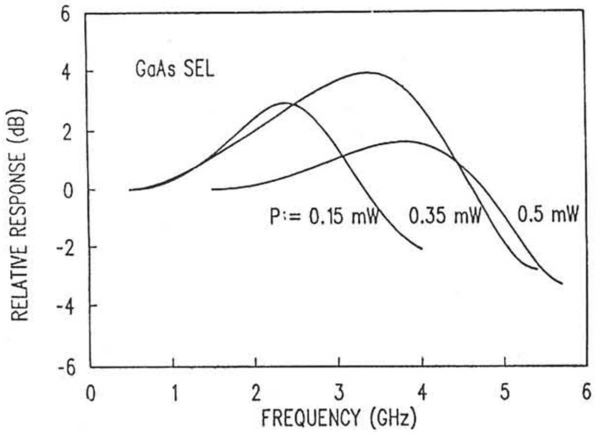

Fig.4.The measured frequency response of the VCSEL at various output power levels.

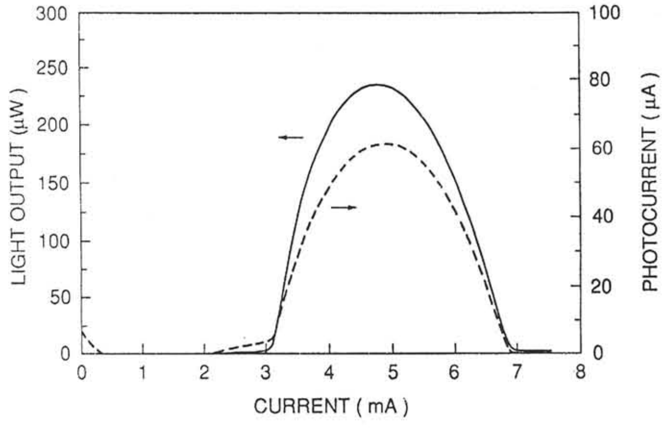

Fig.5 L-I characteristics of the top emitting SEL under room temperature CW conditions. Dotted curve represents the corrected photocurrent of the integrated PIN photodetector.